Int. J. Solids Structures Vol. 26, No. 9/10, pp. 1115–1131, 1990
Printed in Great Britain.

0020–7683/90 $3.00 + .00
Pergamon Press plc

ON GLOBAL SHEAR TRANSFER ACROSS A CRACK OR JOINT PLANE PENETRATED BY CONTINUOUS FIBER REINFORCEMENT WITH APPLICATION TO REINFORCED CONCRETE

G. A. HEGEMIER and H. MURAKAMI
Department of Applied Mechanics and Engineering Sciences, University of California, San Diego, La Jolla, CA 92093, U.S.A.

Abstract—Although this paper focuses on reinforced concrete, the underlying theoretical problem is common to many modeling problems associated with the nonlinear response of brittle matrix, fiber-reinforced composite materials. This class of composites includes structural materials such as reinforced concrete and reinforced concrete masonry, and advanced materials such as carbon/carbon and fiber-reinforced ceramic composites. The problem common to these material types is the prediction of the overall shear resultant transmitted across an interface, the plane of which is penetrated by reinforcing "fibers". In practice, this plane may represent a construction joint, the intersection of two wall elements, or a crack. The most difficult segment of the modeling problem is the treatment of that part of the resultant force which is contributed by the fibers. Within the context of reinforced concrete, this is the classical "dowel action" problem. In what follows, a theoretical description of dowel action is developed for the case of an interface which is normal to the principal direction of reinforcement. This description incorporates dowel action, nonlinear axial dowel effects, interface shear transfer, and bond action. Model validation is accomplished by comparing experimental data with theoretical predictions for a variety of cases involving both monotonic and hysteretic loadings. It is emphasized that the resulting model is largely non-phenomenological. In view of the interactive nature of the basic mechanisms involved in dowel action problems, such a description is needed to properly understand and utilize test data.

1. INTRODUCTION

The nonlinear global response of fiber-reinforced brittle-matrix composites, ranging from structural materials such as reinforced concrete to advanced materials such as reinforced ceramics, is often dominated by complex mechanisms associated with fiber–matrix interactions. Within the context of the former composite, these mechanisms include interface shear transfer (IST), dowel action (DA), nonlinear dowel effects (NDE), and fiber–matrix bond action (BA). While the terminology may vary for other composites, the aforementioned mechanisms are basically similar.

The fiber–matrix interaction mechanisms noted above are, in general, interdependent. This interdependence places a severe limitation on experimental attempts to quantify the contribution of each mechanism. Such experimental difficulties are amplified by a dependence of test data on the test set-up, i.e. on the particular boundary value problem under consideration. For example, in the case of reinforced concrete, Fenwick and Paulay (1968) have shown that the measured global force versus displacement relations from DA and DA plus IST tests depend strongly on the geometry of the test specimen and the test set-up, i.e. on structural constraints. The inability to separate structural effects and basic material properties within a framework of continuum mechanics renders the development of empirical relations for the response of composite structural members of arbitrary geometry and boundary conditions intractable.

Problems such as those noted above demonstrate the need for analytical descriptions of the basic fiber–matrix interaction mechanisms. Even one-dimensional analytical models (Friberg, 1940; Rehm, 1961; Hegemier *et al.*, 1985) have proved to be very helpful in studies of certain coupled interaction mechanisms in composites such as reinforced concrete.

To achieve optimum utility and simulation capability, analytical descriptions such as those noted above should be nonphenomenological. In particular, the global behavior of a composite member should be synthesized from the properties and geometries of the basic composite components (fibers, matrix, interfaces). Further, the description should provide measures of local fields (e.g. average stress states at interfaces, interface slip, etc.) as well as global fields.

SAS 26:9/10-J

The development of an analytical model of fiber-reinforced brittle-matrix composites that can *synthesize* global behavior from component responses is a difficult task which requires some level of micromechanical analysis. This is especially true when a DA-type mechanism is active. In this paper, one procedure for accomplishing this task is discussed and a specific problem is considered. The latter involves combined DA, NDE, IST and BA. This work represents a generalization of a linear dowel action model (Murakami and Hegemier, 1986) to include large deflections, moderately large rotations, and small-strain plastic deformation of the reinforcements. As a result, and in contrast to the previous work, the resulting analytical description is capable of simulating large slip dowel tests (e.g. see Karagozian and Case, 1973; Paulay *et al.*, 1974).

Following model development, the simulation capability of the theory is demonstrated for both monotonic and hysteretic dowel-deformation–time histories. The monotonic cases are conducted with and without IST. The hysteretic example excludes IST; BA and NDE effects are included in all examples. The composite treated is reinforced concrete.

The discussion herein focuses on a special case of a more general problem. In particular, the crack or joint plane is assumed to be normal to the principal reinforcement direction. The general case where such planes occur at arbitrary angles with respect to the principal reinforcement directions will be treated in a subsequent work.

2. FORMULATION

Consider a unidirectional reinforced brittle matrix composite element of length $2l$ with a *pre-existing* matrix crack or joint plane which is normal to the reinforcement at the center of the undeformed specimen. (This element may represent an actual structure or a "cell" in a periodic undirectional fiber layout, see Murakami and Hegemier, 1986.) Let rectangular Cartesian coordinates X_1, X_2, X_3 be selected with X_1 in the axial (fiber) direction as shown in Fig. 1. The crack surface in the undeformed configuration is thus located at $X_1 = 0$. For notational convenience, $(\ )^{(\alpha)}$, $\alpha = 1, 2$, will denote quantities associated with material α with $\alpha = 1$ representing the fiber and $\alpha = 2$ the matrix. In the cross-sectional X_2, X_3-plane the fiber center is located at the origin of the coordinates, and material α occupies the domain $A^{(\alpha)}$; the exterior boundary of $A^{(1)} \cup A^{(2)}$ and the interface between the fiber and matrix are denoted by ∂A and I, respectively.

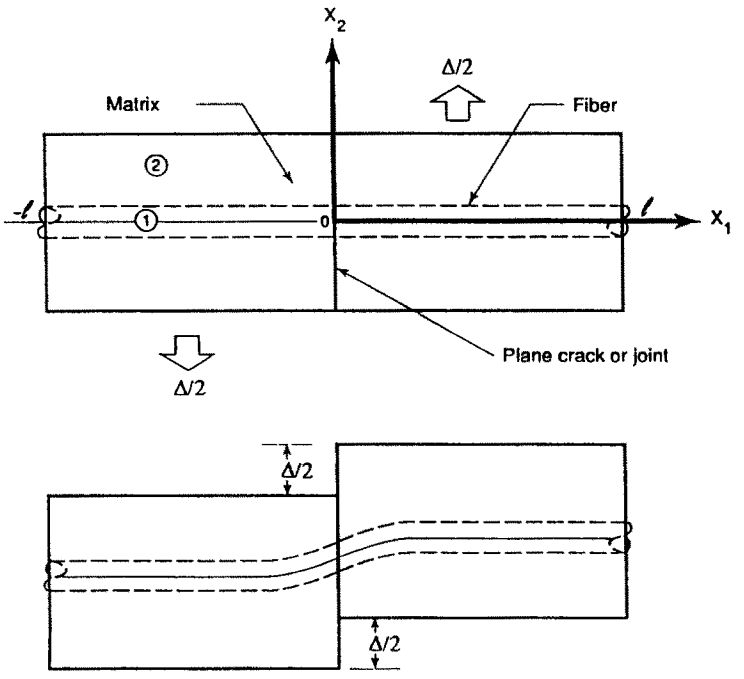

Fig. 1. Geometry and coordinate system.

In what follows, a dowel-type problem will be considered for which the displacements on ∂A are prescribed as depicted in Fig. 1. For a given history, the corresponding global forces in the coordinate directions are sought, as well as details concerning the stress states in material α.

Model construction for DA

A model for deformation in the X_1, X_2-plane is developed by application of a direct variational method in conjunction with an appropriate trial displacement field, and by invoking an approximation of plane stress in the X_1, X_2-plane at a certain point of the analysis. Both the trial functions and the plane stress assumption have been previously adopted in the derivations of classical beam-type theories.

Analysis of the dowel problem commences by application of the principle of virtual work to each material in the undeformed configuration. Addition of the results furnishes

$$\int_0^l \int_{\partial A_T} \overset{v}{T}{}_i^{(2)} \delta u_i^{(2)} \, ds_0 \, dX_1 + \left[\sum_{\alpha=1}^{2} \int\int_{A^{(\alpha)}} \overset{1}{T}{}_i^{(\alpha)} \delta u_i^{(\alpha)} \, dX_2 \, dX_3 \right]_{X_1=0}^{X_1=l}$$
$$= \int_0^l \left\{ \sum_{\alpha=1}^{2} \int\int_{A^{(\alpha)}} S_{ij}^{(\alpha)} \delta E_{ij}^{(\alpha)} \, dX_2 \, dX_3 + \oint_I \overset{v}{T}{}_i^{*} \delta[u_i] \, ds_0 \right\} dX_1, \quad (1)$$

where $S_{ij}^{(\alpha)}$ is the second Piola–Kirchhoff stress, $E_{ij}^{(\alpha)}$ is the Green–Lagrange strain, $u_i^{(\alpha)}$ is the displacement, $[u_i] = u_i^{(2)} - u_i^{(1)}$ is the displacement discontinuity (slip) at the surface I, $\overset{v}{T}{}_i$ is the stress vector defined on the surface with exterior normal v_i, and $\overset{v}{T}{}_i^{*}$ denotes the stress vector on I; both $\overset{v}{T}{}_i$ and $\overset{v}{T}{}_i^{*}$ are defined in the undeformed configuration. In (1) the virtual displacement and strain are expressed by δu_i and δE_{ij}, respectively, and ds_0 denotes the infinitesimal line element on ∂A_T and I; the quantity ∂A_T denotes the subdomain of ∂A on which the traction is specified.

In the development it is assumed that the fiber experiences large deflections and moderate rotations with small strain plastic deformation. At the interface I, the fiber–matrix interface is allowed to suffer relative axial slip $[u_1]$; the matrix in the neighborhood of I may experience cracking or crushing due to the relative transverse displacement $[u_2]$ between the fiber and matrix. The interface I is an "effective" surface associated with a fiber that may be deformed in some applications, e.g. in the case of reinforced concrete.

The assumed trial displacement field for use in (1) has the form

$$u_i^{(\alpha)}(X_1, X_2, X_3) = U_i^{(\alpha)}(X_1) + \delta_{i1} \psi_1^{(\alpha)}(X_1) X_2, \quad (2)$$

where δ_{ij} is the Kronecker delta.

Under (2), the Green–Lagrange strains become

$$E_{11}^{(\alpha)} = U_{1,1}^{(\alpha)} + \psi_{1,1}^{(\alpha)} X_2 + \tfrac{1}{2}(U_{2,1}^{(\alpha)})^2, \quad E_{22}^{(\alpha)} = 0,$$
$$E_{12}^{(\alpha)} = \tfrac{1}{2}(U_{2,1}^{(\alpha)} + \psi_1^{(\alpha)}). \quad (3)$$

For simplicity, and to be consistent with the premise of moderate rotations, the von Karman approximation (von Karman, 1910) has been adopted in which only the nonlinear terms associated with $U_{2,1}$ have been retained in (3).

Substitution of (2) and (3) into (1) and integration by parts furnishes

$$\int_0^l \{[N_{11,1}^{(\alpha)} + (-1)^{\alpha+1} P_1 + \delta_{\alpha 2} Q_1] \delta U_1^{(\alpha)} + [(N_{12}^{(\alpha)} + U_{2,1}^{(\alpha)} N_{11}^{(\alpha)})_{,1}$$
$$+ (-1)^{\alpha+1}(P_2 + U_{2,1}^{(\alpha)} P_1) + \delta_{\alpha 2}(Q_2 + U_{2,1}^{(\alpha)} Q_1)] \delta U_2^{(\alpha)}$$
$$+ [M_{11,1}^{(\alpha)} - N_{12}^{(\alpha)} + (-1)^{\alpha+1} P_1^{II} + \delta_{\alpha 2} Q_1^{II}] \delta \psi_1^{(\alpha)} \} \, dX_1$$
$$- \Big[(N_{11}^{(\alpha)} - \overset{1}{T}{}_1^{(\alpha a)}) \delta U_1^{(\alpha)} + (N_{12}^{(\alpha)} + U_{2,1}^{(\alpha)} N_{11}^{(\alpha)} - \overset{1}{T}{}_2^{(\alpha a)}) \delta U_2^{(\alpha)}$$
$$+ (M_{11}^{(\alpha)} - \overset{1}{T}{}_1^{II(\alpha a)}) \delta \psi_1^{(\alpha)} \Big]_{X_1=0}^{X_1=l} = 0, \quad (4)$$

where

$$[N_{11}, N_{12}, M_{11}]^{(\alpha)} \equiv \int\int_{A^{(\alpha)}} [S_{11}, S_{12}, X_2 S_{11}]^{(\alpha)} \, dX_2 \, dX_3, \tag{5a}$$

$$[P_1, P_2, P_1^{II}] \equiv \oint_I \left[\overset{v}{T}{}_1^{(K)}, \overset{v}{T}{}_2^{(K)}, X_2 \overset{v}{T}{}_1^{(K)} \right]^* ds_0, \tag{5b}$$

$$\left[\overset{1}{T}{}_1^{(\alpha a)}, \overset{1}{T}{}_2^{(\alpha a)}, \overset{1}{T}{}_1^{II(\alpha a)} \right] \equiv \int\int_{A^{(\alpha)}} \left[\overset{1}{T}{}_1^{(\alpha)}, \overset{1}{T}{}_2^{(\alpha)}, X_2 \overset{1}{T}{}_1^{(\alpha)} \right] dX_2 \, dX_3, \tag{5c}$$

$$[Q_1, Q_2, Q_1^{II}] \equiv \oint_{\partial A_T} \left[\overset{v}{T}{}_1^{(K)}, \overset{v}{T}{}_2^{(K)}, X_2 \overset{v}{T}{}_1^{(K)} \right] ds_0 \tag{5d}$$

and where [ ]* implies that [ ] is evaluated on the interface I of the undeformed configuration.

In the derivation of (4), the following expressions were employed:

$$\overset{v}{T}{}_i^* = T_{ji} v_j = \frac{\partial x_i}{\partial X_k} S_{jk} v_j = \frac{\partial x_i}{\partial X_k} \overset{v}{T}{}_k^{(K)}, \tag{6a}$$

$$\overset{1}{T}{}_i^{(\alpha)} = T_{1i}^{(\alpha)} = \frac{\partial x_i}{\partial X_k} S_{1k}, \tag{6b}$$

where T_{ij} is the *first* Piola–Kirchhoff stress and $\overset{v}{T}{}_k^{(K)} = S_{jk} v_j$ is the stress vector related to the *second* Piola–Kirchhoff stress. In the spirit of the von Karman approximation for moderate rotations, the undeformed coordinates X_k were related to the deformed coordinates x_i by

$$\begin{aligned} &\partial x_1/\partial X_1 = 1, \quad \partial x_1/\partial X_2 = 0 \\ &\partial x_2/\partial X_1 = U_{2,1}, \quad \partial x_2/\partial X_2 = 1. \end{aligned} \tag{6c}$$

Equation (4) indicates that the Euler–Lagrange relations of the variational problem on $0 < X_1 < l$ are:

$$\text{either } \delta U_1^{(\alpha)} \equiv 0 \quad \text{or} \quad N_{11,1}^{(\alpha)} + (-1)^{\alpha+1} P_1 + \delta_{\alpha 2} Q_1 = 0, \tag{7a}$$

$$\text{either } \delta U_2^{(\alpha)} \equiv 0 \quad \text{or} \quad N_{11}^{(\alpha)} U_{2,11}^{(\alpha)} + N_{12,1}^{(\alpha)} + (-1)^{\alpha+1} P_2 + \delta_{\alpha 2} Q_2 = 0, \tag{7b}$$

$$\text{either } \delta \psi_1^{(\alpha)} \equiv 0 \quad \text{or} \quad M_{11,1}^{(\alpha)} - N_{12}^{(\alpha)} + (-1)^{\alpha+1} P_1^{II} + \delta_{\alpha 2} Q_1^{II} = 0, \tag{7c}$$

where (7a) was used to simplify (7b). In addition, the appropriate boundary conditions to (7) at $X_1 = 0$ and $X_1 = \pm l$ are

$$\text{either } \delta U_1^{(\alpha)} = 0 \quad \text{or} \quad N_{11}^{(\alpha)} = \overset{1}{T}{}_1^{(\alpha a)}, \tag{8a}$$

$$\text{either } \delta U_2^{(\alpha)} = 0 \quad \text{or} \quad [N_{12}^{(\alpha)} + U_{2,1}^{(\alpha)} N_{11}^{(\alpha)}] = \overset{1}{T}{}_2^{(\alpha a)} \tag{8b}$$

$$\text{either } \delta \psi_1^{(\alpha)} = 0 \quad \text{or} \quad M_{11}^{(\alpha)} = \overset{1}{T}{}_1^{II(\alpha a)}. \tag{8c}$$

Equations (7) are of the *mixture* form. The quantities P_1, P_2, P_1^{II} are *interaction* terms, which reflect stress transfer between the fiber and matrix across the interface I. The quantities Q_1, Q_2, Q_1^{II} denote forces or moments resulting from tractions on the *exterior* cell boundary ∂A_T.

In the remainder of the analysis, attention is focused on a special dowel problem for which

$$U_1^{(2)} = 0, \quad U_2^{(2)} = \operatorname{sgn}(X_1)\Delta/2, \quad \psi_1^{(2)} = 0 \tag{9}$$

where $\operatorname{sgn}(X_1) = 1$ for $X_1 > 0$ and $= -1$ for $X_1 < 0$. This case corresponds to a *uniform* displacement of the exterior boundary ∂A of the matrix cover (see Fig. 1). Under (9) $\delta U_i^{(2)} = 0$ on $0 < X_1 < l$, and the relevant mixture relations reduce to

$$N_{11,1}^{(1)} + P_1 = 0, \tag{10a}$$

$$N_{12,1}^{(1)} + N_{11}^{(1)} U_{2,11}^{(1)} + P_2 = 0, \tag{10b}$$

$$M_{11,1}^{(1)} - N_{12}^{(1)} + P_1^{II} = 0 \tag{10c}$$

on $0 < X_1 < l$ and

$$\text{either } \delta U_1^{(1)} = 0 \quad \text{or} \quad N_{11}^{(1)} = \overset{1}{T}{}_1^{(1a)}, \tag{11a}$$

$$\text{either } \delta U_2^{(1)} = 0 \quad \text{or} \quad [N_{12}^{(1)} + U_{2,1}^{(1)} N_{11}^{(1)}] = \overset{1}{T}{}_2^{(1a)}, \tag{11b}$$

$$\text{either } \delta \psi_1^{(1)} = 0 \quad \text{or} \quad M_{11}^{(1)} = \overset{1}{T}{}_1^{II(1a)}, \tag{11c}$$

on $X_1 = 0, l$.

For the case of DA only, a lubricated interface is assumed at $X_1 = 0$. Further, a test set-up is considered for which the matrix is traction free at the termini $X_1 = \pm l$. This condition corresponds to

$$\overset{1}{T}{}_2^{(2a)} = 0 \quad \text{at} \quad X_1 = 0, \pm l \tag{12a}$$

$$\overset{1}{T}{}_1^{(2a)} = 0 \quad \text{at} \quad X_1 = 0, \pm l. \tag{12b}$$

In addition to (10), constitutive relations are required for $N_{11}^{(1)}$, $N_{12}^{(1)}$, $M_{11}^{(1)}$, P_1, P_2, P_1^{II} to close the model. For this purpose it is necessary to relate the time rate of change of the second Piola–Kirchhoff stress $\dot{\mathbf{S}}$ and the time rate of change of the Green–Lagrange strain $\dot{\mathbf{E}} \equiv \partial \mathbf{E}/\partial t$ at the time t to the corresponding quantities in the deformed configuration. For *small strain* problems it is possible to interpret the components of $\mathbf{S}$ as those of the Cauchy stress $\boldsymbol{\sigma}$ with respect to the covariant bases, and the components of $\dot{\mathbf{E}}$ as those of the rate of deformation tensor $\mathbf{D}$, with respect to the convected contravariant bases in the deformed configuration. The premise of small strain implies that the convected covariant bases ($\mathbf{g}_1$, $\mathbf{g}_2$) can be approximated by the rotated rectangular Cartesian bases ($\mathbf{g}_1^*$, $\mathbf{g}_2^*$) at $X_2 = 0$, one of which is $\mathbf{g}_1$ and the other orthogonal to $\mathbf{g}_1$ to form a right-handed system, Fig. 2. As a result of these approximations, one may interpret $N_{ij}^{(1)}$, $M_{11}^{(1)}$, P_i and P_1^{II} as the corresponding quantities defined in terms of the Cauchy stress with respect to rotated rectangular Cartesian bases.

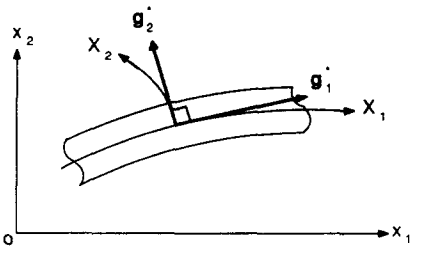

Fig. 2. Base vectors.

For elastic response, the appropriate *stress* constitutive relations are, under the approximation of plane stress in the X_1, X_2 plane,

$$\dot{S}_{11}^{(1)} = E^{(1)}\dot{E}_{11}^{(1)}, \tag{13a}$$

$$\dot{S}_{12}^{(1)} = 2\mu^{(1)}\dot{E}_{12}^{(1)}. \tag{13b}$$

Substitution of (13) into (5a) with use of (3) for $\alpha = 1$ furnishes the elastic segment of the constitutive relations in the form:

$$\dot{N}_{11}^{(1)} = n^{(1)}E^{(1)}A(\dot{U}_{1,1}^{(1)} + U_{2,1}^{(1)}\dot{U}_{2,1}^{(1)}), \tag{14a}$$

$$\dot{N}_{12}^{(1)} = n^{(1)}\mu^{(1)}A(\dot{U}_{2,1}^{(1)} + \dot{\psi}_1^{(1)}), \tag{14b}$$

$$\dot{M}_{11}^{(1)} = E^{(1)}I^{(1)}\dot{\psi}_{1,1}^{(1)} \tag{14c}$$

where $n^{(1)}A$ is the area of the subdomain $A^{(1)}$ and $n^{(1)}$ denotes the area fraction of the fiber in the X_2, X_3-plane, A is the total area of the slip plane, and

$$I^{(1)} \equiv \int\int_{A^{(1)}} (X_2)^2 \, dX_2 \, dX_3. \tag{15}$$

For plastic response of the rebar, the von Mises yield criterion with the associated flow rule is employed with respect to the rotated coordinate bases as follows:

$$f(\boldsymbol{\sigma}) = \sqrt{3J_2} - \sigma_y(\kappa) = 0 \tag{16}$$

where, for plane stress,

$$3J_2 = \sigma_{11}^2 + \tfrac{3}{2}(\sigma_{12}^2 + \sigma_{21}^2) \tag{17}$$

and σ_y is the yield stress in simple tension; the latter is a function of the plastic work κ where

$$\dot{\kappa} = \sigma_{ij}D_{ij}^p. \tag{18}$$

The quantity D_{ij}^p is the plastic part of the rate of deformation tensor. Application of the associated flow law gives

$$D_{11}^P = \frac{\lambda}{\sigma_y}\sigma_{11}, \quad D_{12}^P = \frac{3\lambda}{2\sigma_y}\sigma_{12} \tag{19}$$

where λ is the plastic multiplier. By invoking the consistency condition, λ can be evaluated. By further invoking the premise of small strains, $\boldsymbol{\sigma}$ and $\mathbf{D}$ can be interchanged with $\mathbf{S}$ and $\dot{\mathbf{E}}$, respectively, as was noted previously. Following use of (13) for the elastic part of $\mathbf{D}$, i.e. $\mathbf{D}^e = \mathbf{D} - \mathbf{D}^p$, one obtains the following local constitutive relations:

$$\begin{bmatrix} \dot{S}_{11} \\ \dot{S}_{12} \end{bmatrix}^{(1)} = \frac{1}{\left[1 + \dfrac{ES_{11}^2 + 9\mu S_{12}^2}{\sigma_y^2 H}\right]} \begin{bmatrix} E\left(1 + \dfrac{9\mu S_{12}^2}{\sigma_y^2 H}\right) & \dfrac{-3E\mu S_{11}S_{12}}{\sigma_y^2 H} \\ \dfrac{-3E\mu S_{11}S_{12}}{\sigma_y^2 H} & \mu\left(1 + \dfrac{ES_{11}^2}{\sigma_y^2 H}\right) \end{bmatrix}^{(1)} \begin{bmatrix} \dot{E}_{11} \\ 2\dot{E}_{12} \end{bmatrix}^{(1)} \tag{20}$$

where

$$H \equiv \sigma_y \frac{d\sigma_y}{d\kappa}. \tag{21}$$

Equation (20) can now be employed to furnish constitutive relations for the global quantities $N_{11}^{(1)}$, $N_{12}^{(1)}$ and $M_{11}^{(1)}$ by substitution into (5a). To facilitate the resulting integrations, and in order to arrive at a result of practical utility, three approximations are made prior to integration. The first consists of dropping terms of $O(S_{12}^2)$ compared to unity in the diagonal elements and denominator of (20); the second consists of approximating σ_y^2 by S_{11}^2 in (20), i.e. assuming $S_{12}^2 \ll S_{11}^2$; the third involves the assumption that the cross-section is *fully* plastic. The result of these approximations, which are judged to be reasonable for the problem class under consideration, is

$$\begin{bmatrix} \dot{N}_{11} \\ \dot{N}_{12} \\ \dot{M}_{11} \end{bmatrix}^{(1)} = \begin{bmatrix} C_{11} & C_{12} & 0 \\ C_{12} & C_{22} & 0 \\ 0 & 0 & C_{33} \end{bmatrix} \begin{bmatrix} \dot{U}_{1,1} + U_{2,1}\dot{U}_{2,1} \\ \dot{U}_{2,1} + \dot{\psi}_1 \\ \dot{\psi}_{1,1} \end{bmatrix}^{(1)} \tag{22}$$

where

$$C_{11} = \frac{E^{(1)}H}{E^{(1)}+H} n^{(1)}A, \quad C_{12} = \frac{-3\mu^{(1)}N_{12}^{(1)}}{\sigma_y(E^{(1)}+H)}$$

$$C_{22} = \mu^{(1)}n^{(1)}A, \quad C_{33} = \frac{E^{(1)}HI^{(1)}}{E^{(1)}+H}. \tag{23}$$

The quantity $E^{(1)}H/(E^{(1)}+H)$ in (23) is the elasto-plastic tangent modulus. The relation (22) was obtained with the aid of a quadratic interpolation of S_{12} over the cross-section $A^{(1)}$, i.e.

$$S_{12}^{(1)} = \gamma N_{12}^{(1)}(a^2 - X_2^2), \quad \frac{1}{\gamma} \equiv \int\int_{A^{(1)}} (a^2 - X_2^2)\, dX_2\, dX_3 \tag{24}$$

where a is the radius of the domain $A^{(1)}$.

In addition to the foregoing global stress constitutive relations, expressions must be considered that define the constitutive behavior of the *interaction* terms $P_i (i = 1, 2)$. Here the P_i, e.g. in (10a) and (10b), represent the forces exerted on the fiber by the matrix. In general, one may write

$$P_i = \mathscr{F}_i([u^i]) \tag{25}$$

where $\mathscr{F}_i$ denote functionals and

$$[u^1] = [U_1] + U_{2,1}^{(1)}[U_2], \quad [u^2] = -U_{2,1}[U_1] + [U_2]. \tag{26a}$$

For the present problem

$$[U_i] \equiv \delta_{i2}\, \mathrm{sgn}\,(X_2)\Delta/2 - U_i^{(1)} \tag{26b}$$

where δ_{ij} is the Kroneker delta and $U_i^{(\alpha)}$ is given in (2). In (26), $[U_i]$ is the interface displacement discontinuity defined in the undeformed configuration; the transformation (26a) has been introduced such that $[u^i]$ are components with respect to the rotated coordinate bases in the deformed configuration.

The interaction term P_1 in (10a) reflects "bond" action between the fiber and matrix, and represents a tangential force on the fiber due to the matrix. In previous studies by Hegemier *et al.* (1985) and Hageman *et al.* (1986) it was found that this interaction term can be adequately expressed in the form

$$\dot{P}_1 = K_1[\dot{u}^1] \tag{27}$$

where K_1 denotes a (nonconstant) tangent modulus. For *monotonic* deformation, the following bilinear form of (27) has been found to be useful:

$$\dot{P}_1 = \beta_1[\dot{u}^1] \quad \text{for} \quad |P_1| \leqslant (P_1)_y,$$
$$\dot{P}_1 = \beta_1^{ep}[\dot{u}^1] \quad \text{for} \quad |P_1| > (P_1)_y \tag{28a}$$

where $(P_1)_y$ denotes a critical value at which the modulus changes from β_1 to β_1^{ep}. If one introduces the hardening parameter H_1, then β_1^{ep} can be written as

$$\beta_1^{ep} = \beta_1\left(1 - \frac{\beta_1}{\beta_1 + H_1}\right). \tag{28b}$$

The constant β_1 in (28), which corresponds to zero bond slip (perfect bond), has been evaluated *analytically* in a previous work by Murakami and Hegemier (1986). For dowel problems involving hysteretic bond slip, a more complex representation of K_1 in (27) is necessary. The form used for computational purposes herein is depicted in Fig. 3.

The interaction term P_2 reflects a normal force on the fiber due to the matrix. Again, for monotonic deformation the bilinear expression below has been adopted

$$\dot{P}_2 = \beta_2[\dot{u}^2] \quad \text{for} \quad |P_2| \leqslant (P_2)_y$$
$$\dot{P}_2 = \beta_2^{ep}[\dot{u}^2] \quad \text{for} \quad |P_2| > (P_2)_y \tag{28c}$$

where

$$\beta_2^{ep} = \beta_2\left(1 - \frac{\beta_2}{\beta_2 + H_2}\right) \tag{28d}$$

and where β_2 has been evaluated *analytically* in Murakami and Hegemier (1986). For hysteretic deformation, the form of K_2 depicted in Fig. 4 has been found to be adequate; in general, the incremental form

$$\dot{P}_2 = K_2[\dot{u}^2], \tag{28e}$$

where K_2 is a tangent modulus, should suffice for most applications.

It is noted, that in contrast to P_1 where the nonlinear part of the bond behavior must be postulated, the nonlinear part of P_2 should be derivable from the component constitutive behavior and geometry. This, however, requires the conduct of a detailed 3-D microanalysis.

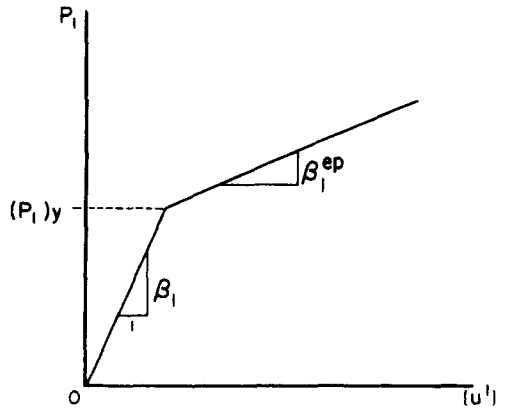

Fig. 3. Interaction term P_1.

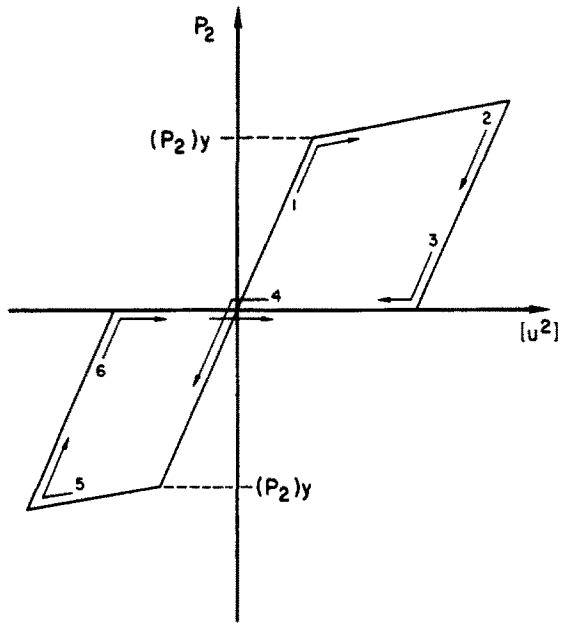

Fig. 4. Interaction term P_2.

This is a formidable task which is outside the scope of the present paper. For purposes of examining the general features of the current modeling process, the constitutive relation for P_2 has been postulated beyond the linear range.

Finally, the interaction term P_1^{II} must be considered. From (5b) it is evident that this quantity represents a moment generated by the fiber–matrix interface shear stress S_{21}. In general, this moment can be shown to be negligible for problems of practical interest which necessitate bond breakage prior to independent bending action of the fiber. As a consequence of this point, it is assumed that

$$P_1^{II} \simeq 0. \tag{29}$$

The formulation of the model is now complete for DA and NDE *without* IST. The basic equations are (10), (14), or (22), (28) and (29), and the boundary conditions (8) with $\alpha = 1$. For convenience, these relations are summarized below; the interaction terms listed refer to the case of monotonic deformation:

Summary of basic equations for DA

(1) Equilibrium:

$$\begin{aligned} &N_{11,1}^{(1)} + P_1 = 0, \\ &N_{12,1}^{(1)} + N_{11}^{(1)} U_{2,11}^{(1)} + P_2 = 0, \\ &M_{11,1}^{(1)} - N_{12}^{(1)} = 0. \end{aligned} \tag{30}$$

(2) Stress constitutive relations:

$$\begin{bmatrix} \dot{N}_{11} \\ \dot{N}_{12} \\ \dot{M}_{11} \end{bmatrix}^{(1)} = \begin{bmatrix} C_{11} & C_{12} & 0 \\ C_{12} & C_{22} & 0 \\ 0 & 0 & C_{33} \end{bmatrix} \begin{bmatrix} \dot{U}_{1,1} + U_{2,1}\dot{U}_{2,1} \\ \dot{U}_{2,1} + \dot{\psi}_1 \\ \dot{\psi}_{1,1} \end{bmatrix}^{(1)} \tag{31a}$$

where

$$C_{11} = E^{(1)}n^{(1)}A, \quad C_{12} = 0, \quad C_{22} = \mu^{(1)}n^{(1)}A, \quad C_{33} = E^{(1)}I^{(1)}$$
$$\text{for} \quad f < 0 \quad \text{or} \quad f = 0 \quad \text{and} \quad \dot{f} < 0 \tag{31b}$$

and

$$C_{11} = \left(\frac{E^{(1)}H}{E^{(1)}+H}\right)n^{(1)}A, \quad C_{12} = -3\left(\frac{\mu^{(1)}}{E^{(1)}+H}\right)\frac{N_{12}^{(1)}}{\sigma_y}, \quad C_{22} = \mu^{(1)}n^{(1)}A,$$

$$C_{33} = \left(\frac{E^{(1)}H}{E^{(1)}+H}\right)I^{(1)} \quad \text{for} \quad f = 0 \quad \text{and} \quad \dot{f} = 0; \tag{31c}$$

in the above,

$$f = \sqrt{3J_2} - \sigma_y, \quad 3J_2 = (N_{11}^{(1)}/n^{(1)}A)^2.$$

(3) Interaction constitutive relations:

$$\dot{P}_i = \beta_i[\dot{u}^i] \quad \text{for} \quad |P_i| \leqslant (P_i)_y$$

$$\dot{P}_i = \beta_i^{ep}[\dot{u}^i] \quad \text{for} \quad |P_i| > (P_i)_y \quad (i = 1, 2, \text{no sum on } i) \tag{32a}$$

where

$$\beta_i^{ep} = \beta_i\left(1 - \frac{\beta_i}{\beta_i + H_i}\right), \tag{32b}$$

$$[u^1] \equiv [U_1] + U_{2,1}^{(1)}[U_2], \quad [u^2] \equiv [U_2] - U_{2,1}^{(1)}[U_1]. \tag{32c}$$

(4) Boundary condition:

$$N_{11}^{(1)} = 0, \quad N_{12}^{(1)} = 0, \quad M_{11}^{(1)} = 0 \quad \text{at } X_1 = \pm l. \tag{33}$$

(5) "Driving" terms:

$$[U_i] = \delta_{i2}\,\text{sgn}\,(X_2)\Delta/2 - U_i^{(1)}. \tag{34}$$

Addition of IST

An elementary procedure for inclusion of IST in the foregoing dowel problem is now considered as follows. First, (30)–(34) are solved incrementally for $U_i^{(1)}$ and $T_i^{(1a)}$ at $X_1 = 0$ where $\overset{1}{T}{}_1^{(1a)} = N_{11}^{(1)}$, $\overset{1}{T}{}_2^{(1a)} = N_{12}^{(1)} + U_{2,1}^{(1)}N_{11}^{(1)}$. Second, an effective normal stress $p = p_0 + \left(\overset{1}{T}{}_1^{(1a)}/A\right)$ is defined on the crack face at $X_1 = 0$, where p_0 is a confining pressure which is part of the test set-up for combined DA+IST experiments. Third, the effective normal stress p is applied to the concrete interface at $X_1 = 0$ and an IST law is postulated in the form $g\left(\overset{1}{T}{}_2^{(2a)}, p, \Delta\right) = 0$ and this relation is solved for $\overset{1}{T}{}_2^{(2a)}$ for a specified p and Δ. This latter quantity reflects IST. According to this procedure, IST influences the total effective shear stress, τ, across $X_1 = 0$ but does not alter the DA contribution, $\overset{1}{T}{}_2^{(1a)}$. Here

$$\tau \equiv \left(\overset{1}{T}{}_2^{(1a)} + \overset{1}{T}{}_2^{(2a)}\right)/A. \tag{35}$$

3. VALIDATION

In this section, the model developed in Section 2 is validated by comparisons between experiments and simulations. This validation is conducted for a number of monotonic and hysteretic cases involving reinforced concrete.

The first case to be considered is a simulation of the lubricated monotonic dowel tests by Paulay *et al.* (1974). The test set-up and specimen are illustrated in Figs 5 and 6. Wax was used to lubricate the joint surface. Comparisons of theoretical and experimental results are shown in Fig. 7 for three different steel volume fractions. Agreement is observed to be good. The "shear stress" in Fig. 7 is based on (35) with $\overset{1}{T}{}_2^{(2a)} = 0$. Simulation of the test, which approximates pure DA, was performed using (30)–(34) and an appropriate incremental numerical procedure. The model parameters employed in the simulation are given in Table 1.

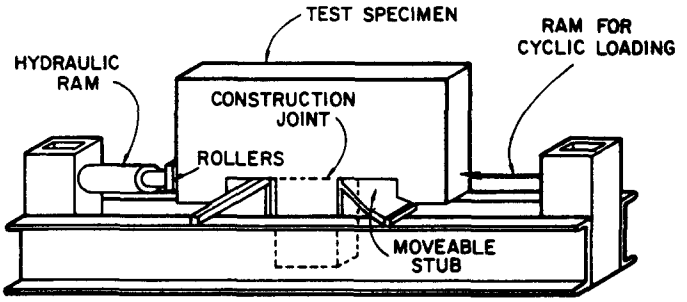

Fig. 5. Test set-up used by Paulay *et al.* (1974).

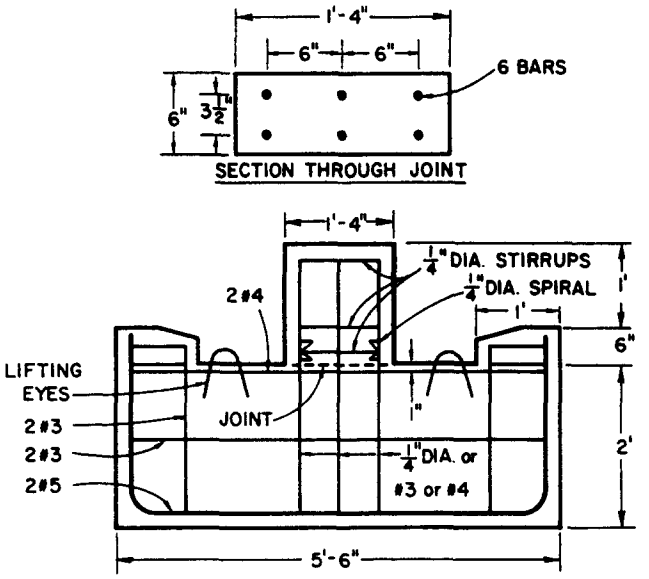

Fig. 6. Test specimen used by Paulay *et al.* (1974).

Table 1. Parameters used in simulation of dowel tests (Paulay *et al.*, 1974)

Parameters / Specimens	$n^{(1)}$	A (in.^{2})	β_1 (psi)	$(P_1)_y$ (lb in.$^{-1}$)	H_1 (psi)	β_2 (psi)	$(P_2)_y$ (lb in.$^{-1}$)	H_2 (psi)	l (in.)
TA01, 02	0.0031	16	2.11×10^6	1850	2×10^5	2.48×10^6	1700	1.2×10^5	2.4
TB01, 02	0.0069	16	2.57×10^6	2770	2×10^5	2.91×10^6	2350	1.2×10^5	4
TC01, 02	0.0123	16	3.03×10^6	3700	2×10^5	3.31×10^6	2800	2.5×10^5	6

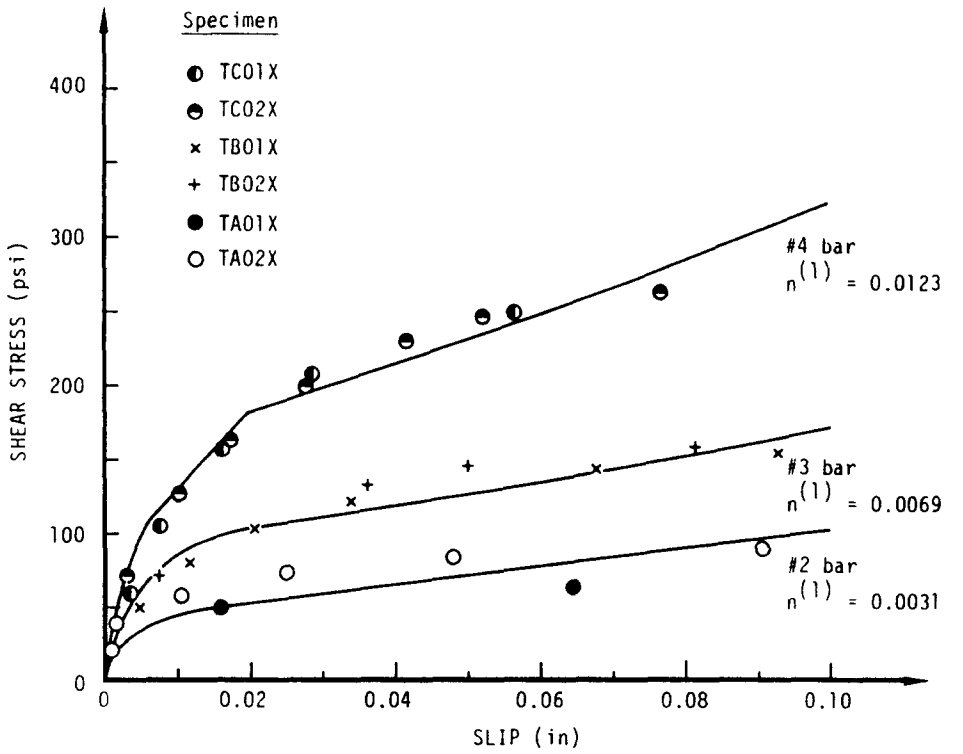

Fig. 7. Comparison of theoretical and experimental results for tests by Paulay *et al.* (1974). Solid lines = simulation.

The second case to be considered includes IST; the tests were performed by Paulay *et al.* (1974) with the test set-up and test specimens of different joint surface preparation which are depicted in Figs 5 and 6. Figure 8 shows comparisons of experimental data and simulations for several different interface conditions. For simulation purposes, an IST relation of the form

$$\overset{1}{T}{}_2^{(2a)}(\Delta)/A = \{\tau_{\max} - \tau_\infty(1-e^{-\gamma})\}\frac{\Delta}{\Delta_y}\exp\frac{1}{\beta}\left\{1-\left(\frac{\Delta}{\Delta_y}\right)^{\beta}\right\}+\tau_\infty\left\{1-\exp\left(-\gamma\frac{\Delta}{\Delta_y}\right)\right\}, \quad (36)$$

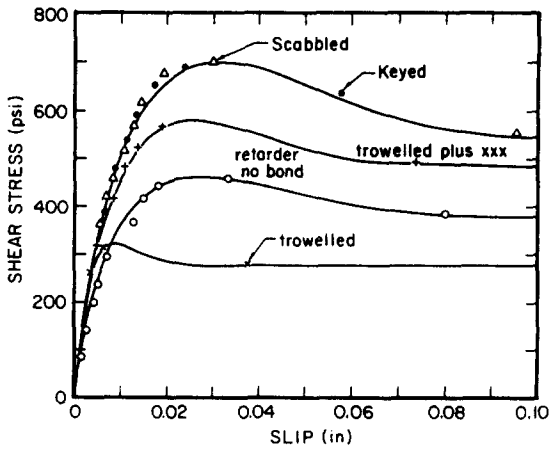

Fig. 8. Comparison of theoretical and experimental results for test by Paulay *et al.* (1974).

Table 2. Parameters used in simulation of IST tests (Pauley *et al.*, 1974)

Parameters / Specimens	β	γ	Δ_c (in.)	τ_{max} (psi)	τ_∞ (psi)
Scabbled, SB01	2.0	4.5	0.03	700	540
Keyed, KB01	2.0	4.5	0.03	700	540
Trowelled plus criss-crossed ZB01	2.0	4.5	0.024	580	480
Retarder, no bond RB01X	2.0	4.5	0.026	460	380
Trowelled, TB01	2.0	4.5	0.008	320	275

was adopted. The model parameters used in the simulation are given in Table 2. Agreement between simulations and test data is observed to be excellent.

Another case of interest concerns the data produced by Karagozian and Case (1973). In these experiments the maximum slip Δ was considerably larger than those associated with the aforementioned tests. The test set-up and specimens used are depicted in Figs 9 and 10. In order to include the effect of confining pressure p on the IST relation (36), τ_{max} and τ_∞ are expressed as:

$$\tau_{max} = 979 + 1.53p \text{ (psi)}$$
$$\tau_\infty = 76 + 0.84p \text{ (psi)}. \tag{37}$$

The remaining model parameters employed for simulation purposes are furnished in Table 3. Comparisons between simulations and test results are illustrated in Fig. 11 for a range of confining pressures. Agreement between predictions and experimental data is observed to be reasonable.

A more critical test of the model simulation capability is represented by the cyclic experiments of Jimenez *et al.* (1978, 1982). The test set-up and specimen are illustrated in Figs 12 and 13. Thin brass sheets were used to lubricate the joint surface. A typical simulation versus experiment is shown in Fig. 14. The agreement is observed to be good considering the complexity of the response. The model parameters employed in the simulation are provided in Table 4.

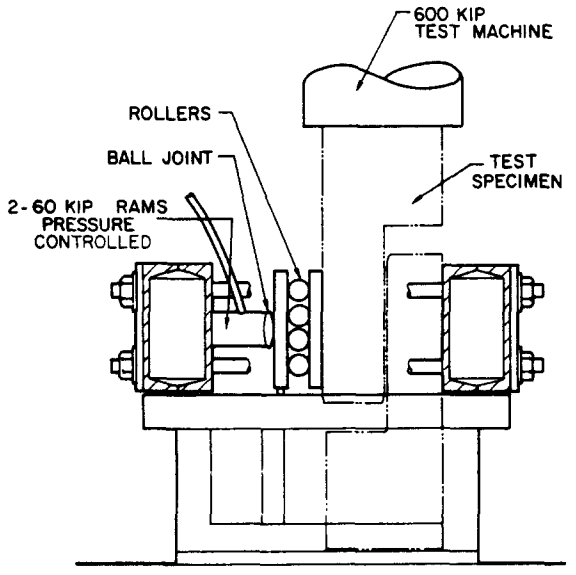

Fig. 9. Test set-up used by Karagozian and Case (1973).

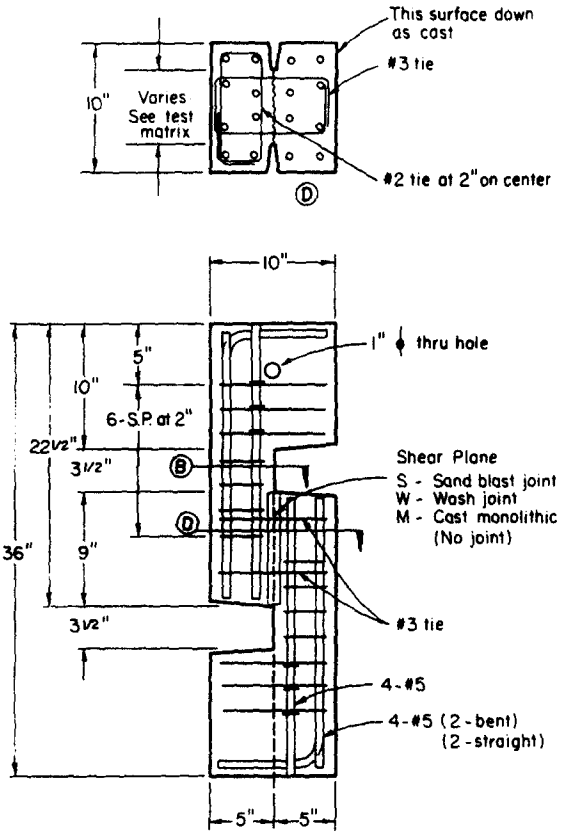

Fig. 10. Test specimen used by Karagozian and Case (1973).

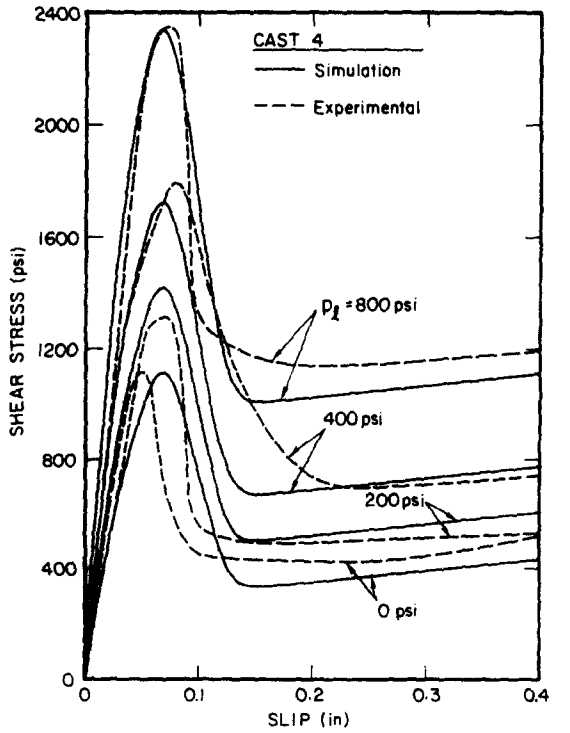

Fig. 11. Comparison of theoretical and experimental results for tests by Karagozian and Case (1973).

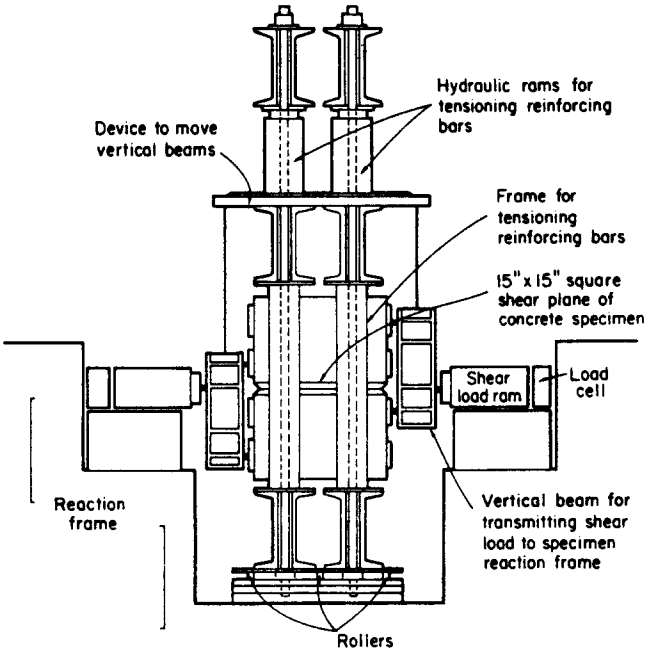

Fig. 12. Test set-up used by Jimenez *et al.* (1978).

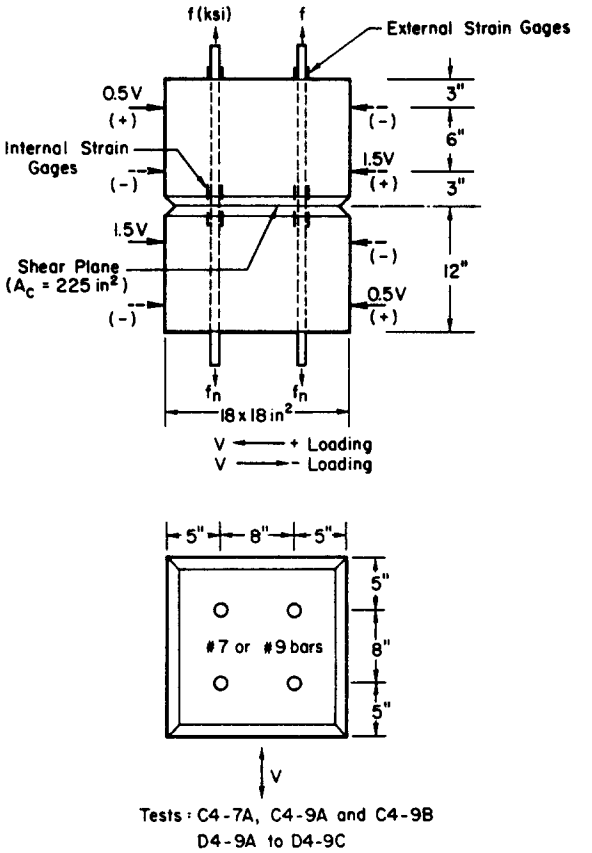

Fig. 13. Test specimen used by Jimenez *et al.* (1978).

Table 3. Parameters used in simulation of tests (Karagozian and Case, 1973)

$n^{(1)}$	A_2 (in.^{2})	$E^{(1)}$ (psi)	$\mu^{(1)}$ (psi)	σ_y (psi)	H (psi)	β_1 (psi)	$(P_1)_y$ (lb in.$^{-1}$)
0.0035	56.25	30×10^6	11×10^6	50×10^3	15×10^3	2.17×10^6	2350

H_1 (psi)	β_2 (psi)	$(P_2)_y$ (lb in.$^{-1}$)	H_2 (psi)	l (in.)	Δ_y (in.)	β	γ
0.338×10^6	2.51×10^6	2500	0.1×10^6	4.0	0.065	4.0	4.5

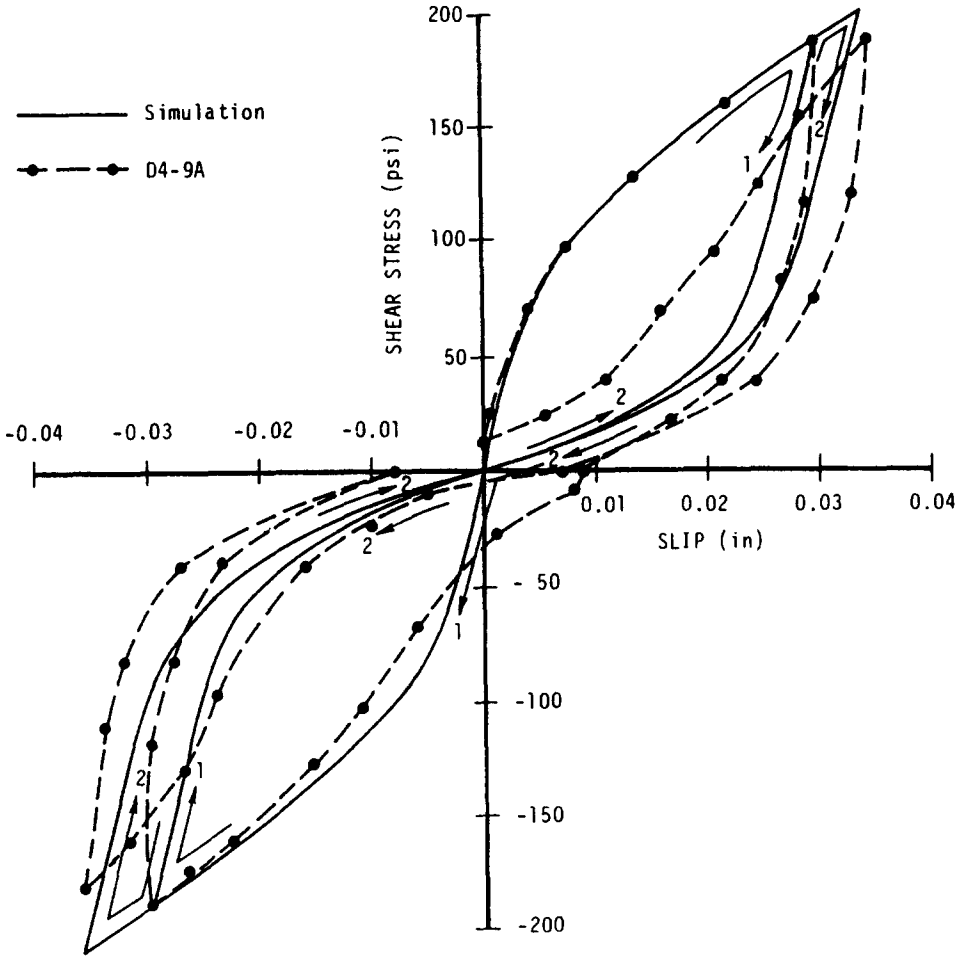

Fig. 14. Comparison of theoretical and experimental results for tests by Jimenez *et al.* (1978).

Table 4. Parameters used in simulation of tests (Jimenez *et al.*, 1978)

Specimen	$n^{(1)}$	A_2 (in.^{2})	$E^{(1)}$ (psi)	$\mu^{(1)}$ (psi)	σ_y (psi)	H (psi)	β_1 (psi)
DA−9A	0.0178	56.25	30×10^6	11×10^6	60×10^3	0.3×10^6	3.41×10^6

β_2 (psi)	$(P_2)_y$ (lb in.$^{-1}$)	H_2 (psi)
3.57×10^6	4500	0.3×10^6

4. CLOSURE

The "dowel problem" concerns the manner in which shear forces are transferred across matrix crack or joint planes in fiber-reinforced composites. Three distinct modes of shear transfer exist across such a plane: (1) interface shear transfer (IST) on the rough surface of the crack or joint; (2) dowel action (DA) in the reinforcement crossing the crack or joint; and (3) components of axial forces in the reinforcing fibers inclined to the crack direction. IST includes the effective frictional and bearing forces generated at a closed or slightly open crack as the protruding particles on each side of the crack surface come into contact. DA is induced by the shear and bending deformations experienced by the reinforcement when shear displacements are applied across the crack. If the dowel transverse displacements become sufficiently large, then axial forces in the fibers crossing the crack also contribute to effective shear resistance.

In this paper, a "dowel model" was constructed for the case in which a single matrix crack or joint occurred normal to the principal reinforcement direction. The model included combined DA and IST as well as bond action (BA) effects, and allowed large dowel deflections with moderate rotations. Using an example composite in the form of reinforced concrete, validation of the model was performed by comparing test data with simulations for both monotonic and hysteretic cases. These comparisons revealed that the dowel model is capable of producing simulations that mirror actual data.

The problem considered herein is a precursor to a more general model formulation for fiber-reinforced, brittle-matrix composites. The latter includes crack or joints which are oblique to the reinforcement.

REFERENCES

Fenwick, R. C. and Paulay, T. (1968). Mechanisms of shear resistance of concrete beams. *J. Struct. Div., ASCE* **94**(ST10), 2325–2350.

Friberg, B. F. (1940). Design of dowels in transverse joints of concrete pavements. *Trans. ASCE*, **105**, 1076–1116.

Hageman, L. J., Murakami, H. and Hegemier, G. A. (1986). On simulating steel–concrete interaction in reinforced concrete, Part II: validation studies, *Mech. Mater.* **5**, 187–197.

Hegemier, G. A., Murakami, H. and Hageman, J. L. (1985). On tension stiffening in reinforced concrete. *Mech. Mater.* **4**, 161–179.

Jimenez, R., Gergely, P. and White, R. N. (1978). Shear transfer across cracks in reinforced concrete. Report No. 78-4, Department of Structural Engineering, Cornell University, Ithaca, NY, NTIS PB-288885/RC.

Jimenez, R., White, R. N. and Gergely, P. (1982). Cyclic shear and dowel action models in R/C. *J. Struct. Div., ASCE* **108**(ST5), 1106–1123.

Karagozian and Case Structural Engineers (1973). Construction joint test program. Final Report for F04701-72-C-0358, submitted to Space and Missile Systems Organization, Air Force Systems Command, Norton AFB, CA.

von Karman, T. (1910). Festigkeits Probleme im Maschinenbau. In *Encyklopädie der Mathematischen Wissenschaften* **IV**(4), Chapter 27.

Murakami, H. and Hegemier, G. A. (1986). On simulating steel-concrete interaction in reinforced concrete, Part I: theoretical development. *Mech. Mater.* **5**, 171–185.

Paulay, T., Park, R. and Phillips, M. H. (1974). Horizontal construction joints in cast-in-place reinforced concrete. ACI Special Publications, SP-42, *Shear in Reinforced Concrete*, **2**, 599–616.

Rehm, G. (1961). *Uber die Grundlager des Verbundes Zwischen Stahl und Beton*, Deutscher Ausschluss für Stahlbeton, H. 138; (1963). *The Basic Principles of the Bond Between Steel and Concrete*. Cement and Concrete Association, Translation No. 134, London.